

**Influence of molecular weight distribution on the melt extrusion of high density polyethylene (HDPE): Effects of melt relaxation behavior on morphology and orientation in HDPE extruded tubular films**

TaHua Yu and Garth L. Wilkes

Citation: *Journal of Rheology* (1978-present) **40**, 1079 (1996); doi: 10.1122/1.550801

View online: <http://dx.doi.org/10.1122/1.550801>

View Table of Contents: <http://scitation.aip.org/content/sor/journal/jor2/40/6?ver=pdfcov>

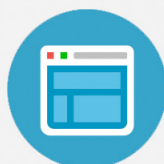
Published by the [The Society of Rheology](#)

---



## Re-register for Table of Content Alerts

Create a profile.



Sign up today!



## **Influence of molecular weight distribution on the melt extrusion of high density polyethylene (HDPE): Effects of melt relaxation behavior on morphology and orientation in HDPE extruded tubular films**

Ta-Hua Yu and Garth L. Wilkes<sup>a)</sup>

*Department of Chemical Engineering, Virginia Polytechnic Institute and State University, Blacksburg, Virginia 24061*

(Received 5 February 1996; final revision received 24 June 1996)

### **Synopsis**

The influence of molecular weight distribution and extrusion processing variables on the morphological features and orientation of high density polyethylene (HDPE) uniaxially extruded tubular films was investigated. In order to gain a better understanding of the orientation–crystallization behavior occurring during extrusion processing, the melt flow properties of the two HDPE resins with identical  $\bar{M}_n$  (14 600) values but different molecular weight distributions ( $\bar{M}_w/\bar{M}_n = 10.3, 15.1$ ), utilized in our previous study, were characterized by dynamic rheological experiments over the temperature range from 150 °C to 230 °C within the angular frequency range from 0.1 to 100 rad/s. The experimental data were shifted to produce master flow curves. The flow activation energy calculated from the shifting process was found to be 25.9 kJ/mol for resin 1 and 29.1 kJ/mol for resin 2. The characteristic relaxation time at 190 °C obtained by use of a Carreau–Yasuda analysis for resin 2 having the broader molecular weight distribution was found to be 6.5 times greater than that of resin 1. This observation further supports our previous conjecture that the prominence of the fibril nuclei in resin 2 is due to its longer melt relaxation time behavior. The extrusion processing variables of melt temperature at the die exit, quench height (which is the distance from the exit of the die to the cooling ring), flow rate of the air through the cooling ring, film line speed, and die gap were varied to control the melt relaxation time of HDPE resins and the processing time frame for cooling. The results show that a longer melt relaxation time and a shorter cooling processing time can enhance the formation of fibril nuclei. The importance of melt relaxation behavior in influencing the final morphological structure in HDPE extruded films and their associated properties is clearly made evident in this paper. © 1996 Society of Rheology.

### **I. INTRODUCTION**

The structural features in extruded films and melt spun fibers are dependent on the molecular behavior such as orientation and crystallization occurring during processing, which in turn are affected by the melt rheological characteristics. Besides processing variables, molecular variables such as molecular weight (MW) and molecular weight distribution (MWD) are also considered to be important for the purposes of controlling flow characteristics [Graessley (1974); Vinogradov and Malkin (1980); Wilkes (1981)]. In 1986, Keller and co-workers investigated the influence of molecular weight distribution on the structural development in melt extruded polyethylene fibers [Bashir *et al.*

<sup>a)</sup>To whom correspondence should be addressed.

(1986)]. Their results showed that the high molecular weight tail is important for controlling the formation of extended chain fibrils in row nucleated structures and this was later explained as due to the fact that the minimum strain rate needed to stretch polymer chains from the random coil state to the fully stretched state (extended conformation) decreases as molecular weight increases [Keller and Kolnaar (1993)]. In more recent work, Spruiell and co-workers studied the structural development and crystallization kinetics of melt spun polypropylene filaments with different molecular weight and molecular weight distribution [Misra *et al.* (1995)]. It was observed that the spinnability, structure, and properties of the polypropylene filaments were strongly influenced by the breadth of molecular weight distribution although no morphological investigations were undertaken. The crystallinity at a given set of spinning conditions and resin melt flow rate were found to increase with a greater polydispersity. According to these findings, they concluded that the major influence of MWD on the structure and properties of polypropylene was due to its effect on both elongational viscosity of the resin and the ability of a high molecular weight tail in the distribution to enhance the stress-induced crystallization that occurs during processing. In our previously reported study [Yu and Wilkes (1996)], the influence of extrusion (uniaxial) process variables on the orientation state and morphology of two high density polyethylene (HDPE) resins (resins 1 and 2) with different molecular weight distributions was investigated. The results suggested that both line stress and the relaxation behavior of an oriented polymer melt are critical in determining the structural features in the extruded films. Specifically, it was found that using the same processing window, the broader molecular weight distribution samples (resin 2), when melt processed into tubular films, possessed fibril nuclei that were not evident for the narrower distribution material (resin 1). The origin of the fibril nuclei observed for the sample with a broader distribution was qualitatively suggested to be due to its expected longer melt relaxation time behavior.

In the 1960s, a theoretical model to predict the viscosity versus shear rate curve was developed by Graessley (1967; 1965). In his model, the Rouse relaxation-time parameter governs the location of the shear rate where the viscosity begins to decrease. The product of the relaxation time constant and the shear rate at the onset of non-Newtonian flow is of the order of unity and is associated with the concept of the Deborah number. This specific relaxation time at which shear thinning begins corresponds to the terminal mode in the corresponding relaxation time spectrum of the polymer chains. Graessley's theory also predicts that viscosity is very sensitive to molecular weight at the beginning of non-Newtonian flow, but it becomes almost independent of molecular weight in the asymptotic shear thinning region with a constant limiting power-law exponent estimated to be 9/11 for narrow distribution systems. Investigations into the dependency of the flow behavior of viscosity versus shear rate on molecular weight distribution have been mostly carried out for polymer solutions [Graessley (1974) (1967); Shroff and Shida (1971)]. Data for melt rheological experiments that address the relaxation time behavior are more limited often due to the narrower frequency window that one can achieve from this approach. In order to quantitatively understand the influence of molecular weight distribution on the melt relaxation time behavior of the two early mentioned HDPE resins, rheological experiments were conducted in this work. The objectives of this study were to (a) determine the difference of the melt flow properties (especially the melt relaxation time at a common temperature) for the two HDPE resins utilized and (b) show that from controlling the degree of melt relaxation time behavior (prior to solidification) by the extrusion variables: the quench height, the melt temperature at the die exit, the quenching rate, the film line speed, and the die gap, the extruded films melt processed from *each of*

**TABLE I.** Molecular weight features of the two HDPE resins.

Sample	$\bar{M}_n$ (g/mol)	$\bar{M}_w$ (g/mol)	$\bar{M}_w/\bar{M}_n$
Resin 1	14 600	150 000	10.3
Resin 2	14 600	219 000	15.1

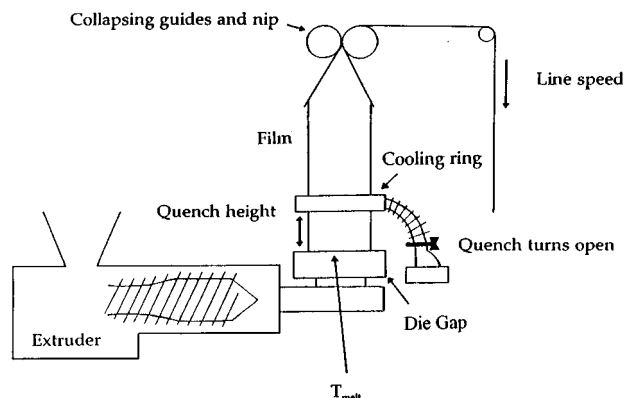
these two resins could be prepared with and without the presence of fibril nuclei structure as determined by transmission electron microscopy (TEM) and WAXS.

## II. EXPERIMENT

Two commercial HDPE resins, designated as resins 1 and 2, were employed in this study. Their molecular weight characteristics that were determined by gel permeation chromatography (GPC) at 135 °C in 1,2-dichlorobenzene are listed in Table I. These two resins were melt extruded through an annular die with a diameter of 12 in. under controlled processing conditions. The process variables investigated are marked on the schematic of the extrusion operation in Fig. 1. The values of the five processing parameters utilized, i.e., the melt temperature,  $T_{\text{melt}}$ , at the die exit, the quench height, which is the distance from the exit of the die to the cooling ring, the flow rate of the air through the cooling ring, the line speed, and the annular die gap are listed in Table II. Again, it is to be noted that the blow-up ratio of unity was utilized for producing *uniaxially* oriented tubular films.

The WAXS analysis of the extruded films was performed by using a Philips tabletop x-ray generator model PW1170 equipped with a standard vacuum sealed Warhus photographic pinhole camera. The nature of the crystalline orientation distribution (orientation function) in uniaxially oriented extruded films can be obtained by examination of the azimuthal angle dependence of different reflections in the x-ray diffraction photographs. The orientation function utilized is the Hermans' orientation function and is given by Hermans *et al.* (1948)

$$f = \frac{\overline{(3 \cos^2 \theta - 1)}}{2} \quad (1)$$

**FIG. 1.** A schematic of the extrusion process.

**TABLE II.** Summary of the extrusion processing variables. Note: Samples A1, A10, and A11 are made from resin 1. Samples B1 and B12 are made from resin 2.

Sample	Melt temperature (°C)	Quench height (in.)	Air flow rate in air ring	Line speed (ft/min)	Die gap (in.)
A1	205	2.5	low	40	0.07
A10	185	1.0	high	80	0.07
A11	185	1.0	high	80	0.14
B1	205	2.5	low	40	0.07
B12	210	3.5	low	40	0.07

in which  $\theta$  is the angle between the chain axis (or a specific crystal unit cell axis) and a chosen reference axis (usually the machine direction). When the orientational unit (chain or crystal axis) is aligned along the reference axis, i.e.,  $\theta = 0^\circ$  for all orientational units,  $f = +1$ , whereas for the case of perpendicular-orientation, i.e.,  $\theta = 90^\circ$ ,  $f = -1/2$ . For random orientation it can be shown that  $f = 0$ . The crystalline chain axis of polyethylene is aligned along the  $c$  axis of the unit cell. Since the  $a$ ,  $b$ , and  $c$  crystallographic axes of polyethylene are not independent, only two of them are necessary in order to completely specify the orientation. For uniaxially oriented polyethylene, it is more convenient to work with the (200) and (020) reflections by Stein's method [Stein (1958) (1964)]. Once the orientation functions of  $a$  and  $b$  axis are obtained, one can calculate the orientation function,  $f_c$ , for the crystalline chain axis using the following relation:

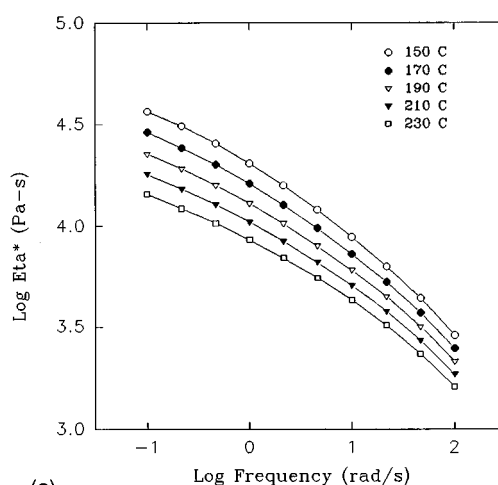
$$f_a + f_b + f_c = 0, \quad (2)$$

where  $f_a$  and  $f_b$  are the orientation functions for the  $a$  and  $b$  axis, respectively. Since we have distinctly shown in our earlier study [Yu and Wilkes (1996)] using WAXS that the extruded tubular films are essentially uniaxially oriented along the machine direction (MD), we have therefore utilized Stein's method [Stein (1958) (1964)] in this study to evaluate the orientation state of the extruded films.

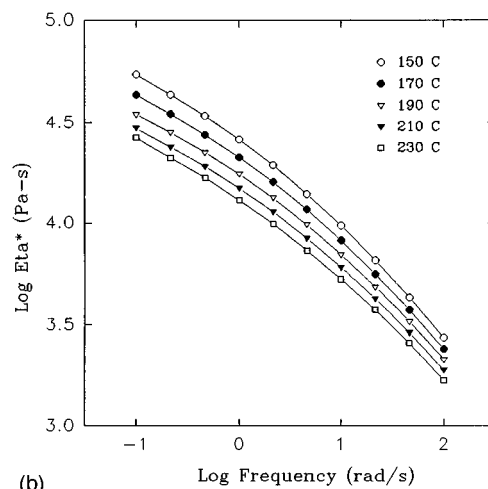
For TEM investigations, the 1-mil-thick extruded films were first treated with chlorosulfonic acid [Grubb and Keller (1980)] at 60 °C for 6 h before microtoming. Thin sections were normally stained on the TEM grid with a dilute aqueous solution of uranyl acetate and then examined by a Philips EM-420 scanning transmission electron microscope (STEM) operated in the transmission mode at 100 kV.

The mechanical properties of some of the extruded films along the MD were measured with an Instron Model 1122 tensile testing machine. The dimensions of the specimens for tensile testing were chosen according to the American Society for Testing and Materials procedure D638. The testing crosshead speed of the Instron was 20 mm/min. The average of five specimens was determined for each sample and reported along with the standard deviation. All measurements were conducted at ambient conditions.

Melt rheological experiments were carried out using a Rheometrics "RMS 800" dynamic rheometer having parallel plates with a diameter of 25 mm. The frequency range covered was from 0.1 to 100 rad/s and the melt temperature range was from 150 °C to 230 °C at intervals of 20 °C. The viscosity data were then shifted to produce isothermal master curves according to the procedure described by Bird *et al.* [Bird *et al.* (1987)]. Flow-activation energy values that describe the dependence of viscosity on temperature were obtained from the shifting process.



(a)



(b)

**FIG. 2.** (a) The complex viscosity as a function of frequency obtained at five temperatures for resin 1. (b) The complex viscosity as a function of frequency obtained at five temperatures for resin 2.

### III. RESULTS AND DISCUSSION

The logarithmic plots of magnitude of the complex viscosity as function of frequency obtained over a range of temperature for both resins are shown in Figs. 2(a) and 2(b). By shifting the viscosity–frequency curves along both the horizontal and vertical axes, master curves of the complex viscosity versus frequency for resins 1 and 2 were constructed at the reference temperature 190 °C as shown in Fig. 3. Flow-activation energy values obtained during the shifting process were 25.9 kJ/mol for resin 1 and 29.1 kJ/mol for resin 2. For *linear* polyethylene, it has been reported that the flow-activation energy is of the order of 25–29 kJ/mol [Vinogradov and Malkin (1980); Tanner (1988)]. This observation provides strong support for the linear chain characteristics for both resins 1 and 2. Further  $^1\text{H}$  and  $^{13}\text{C}$ -NMR analysis [Callahan and Fisher (1995)] of these two resins also supports this same conclusion.

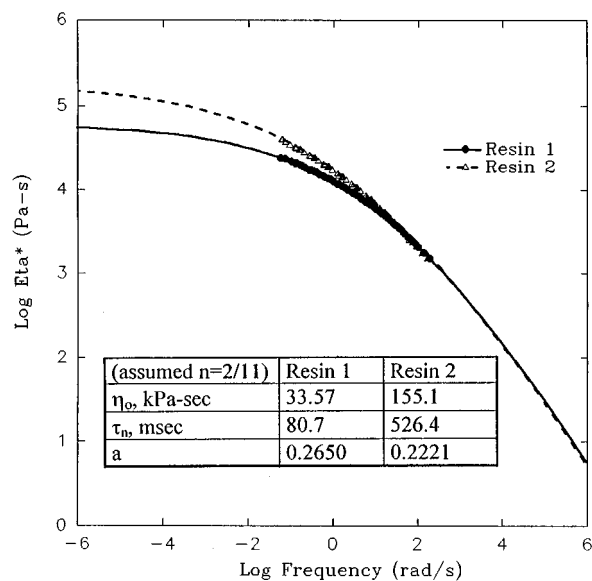
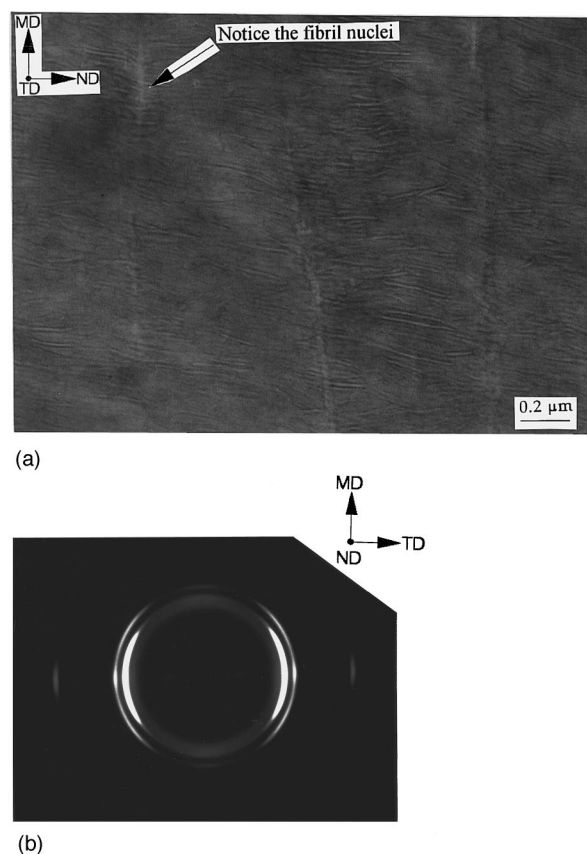


FIG. 3. Isothermal master curves of complex viscosity vs frequency at 190 °C for resins 1 and 2.

Accepting the applicability of the Cox–Merz rule as valid for our system, the resulting master curve was fit with the Carreau–Yasuda equation [Yasuda *et al.* (1981)]

$$|\eta^*(\omega)| = \frac{\eta_0}{[1 + (\omega \cdot \tau)^a]^{1-n/a}}, \quad (3)$$

where  $\eta^*(\omega)$  is the complex viscosity,  $\omega$  is the oscillation frequency,  $\eta_0$  is the zero shear rate viscosity,  $n = 2/11$  is the limiting power-law exponent as suggested by Graessley (1967), “ $a$ ” is a fitting parameter whose value increases with the “sharpness” of the onset of shear thinning, and  $\tau$  is the characteristic relaxation time related to the onset of non-Newtonian or shear thinning behavior. The curves obtained by fitting the isothermal master curves with Eq. (3) are shown as the extrapolated curves in Fig. 3. It is recognized that this model is basically empirical in nature but as will be illustrated, it can provide useful information on the difference in the relaxation behavior of the two resins under comparison. The zero shear rate viscosity ( $\eta_0$ ), the parameter  $a$ , and the relaxation time ( $\tau$ ) obtained during the curve fitting are also included in Fig. 3. As it has been shown by Friedman and Porter (1975), for equal molecular architecture, the Newtonian viscosity of polystyrene and polydimethylsiloxane strongly depends on weight average molecular weight. Similar conclusions have also been obtained by Shaw (1977) for polyethylene and by Cantow (1963) for polystyrene as well as many other polymers of comparable architecture. Therefore, as would be expected, resin 2, which possesses a higher weight average molecular weight than resin 1, has the greater zero shear rate viscosity. The difference in the values of the parameter “ $a$ ” between the two resins is found to be small. As stated above, the parameter “ $a$ ” in the empirical Carreau–Yasuda equation determines the curve shape or breadth of the transition over which the fluid transfers from Newtonian behavior to that of shear thinning. Since resin 2 has a broader molecular weight distribution, a broader transition (or a smaller “ $a$ ” value) was observed as expected for resin 2 in Fig. 3. The most interesting finding in Fig. 3 is that the characteristic



**FIG. 4.** (a) The TEM micrograph for resin 2, sample B1 showing fibril nuclei. (b) The WAXS diffraction pattern for resin 2, sample B1 that possessed fibril nuclei.

relaxation time,  $\tau$ , obtained from the Carreau–Yasuda analysis for resin 2 having the broader molecular weight distribution is found to be 6.5 times greater than that of resin 1. This characteristic relaxation time is an index of the longest molecular relaxation time and clearly shows the influence of the higher molecular weight tail in resin 2.

In our previous study, *the fibril nucleated structure were directly observed by TEM for all the extruded films made from resin 2 that possessed the broader molecular weight distribution.* The *c*-axis crystalline orientation functions for the extruded films made from resin 2, determined by WAXS, varied only from 0.63 to 0.72 over the range of processing variables utilized. The TEM micrograph and WAXS diffraction pattern for the lowest oriented resin 2 extruded film with  $f_c = 0.63$  studied in our previous work, sample B1, are shown in Figs. 4(a) and 4(b), respectively. The highly oriented fibril or row nuclei observed in the TEM micrograph was also confirmed from WAXS by intense sharp (110), (200), and (020) spots superimposed on the equatorial reflections that arose from the remaining less but still quite well oriented stacked lamellae making up the bulk morphology of the film. In contrast to resin 2, *using the same processing window*, none of the extruded films made from resin 1 in our previous work showed morphological evidence of fibril nucleated structure. The crystalline orientation functions, evaluated by WAXS, for resin 1 extruded films varied from 0.45 to 0.67. It is noted that the upper end of the orientation functions for resin 1 overlaps with the lower end of the orientation functions



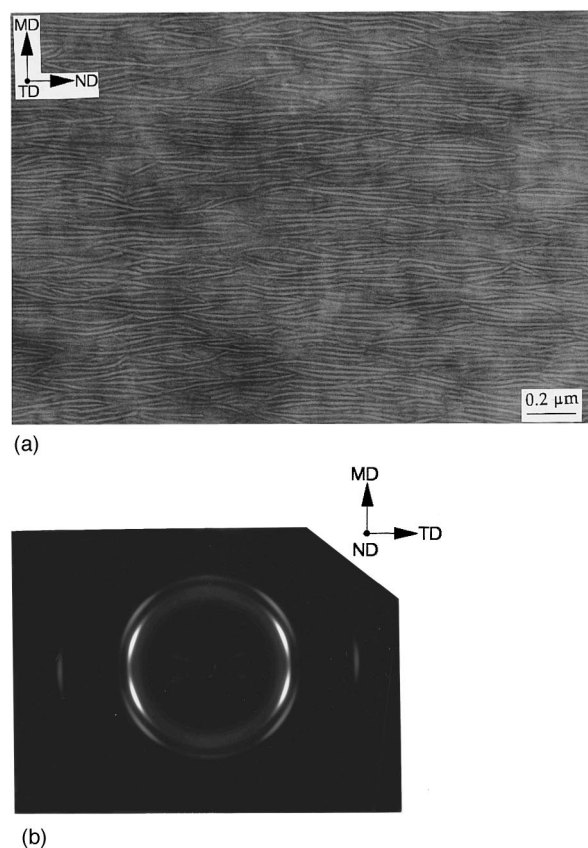
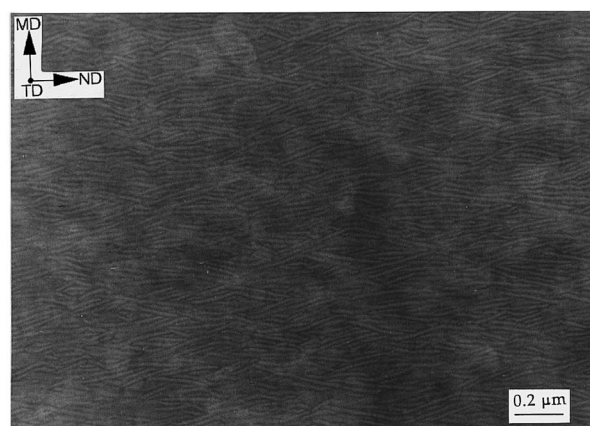
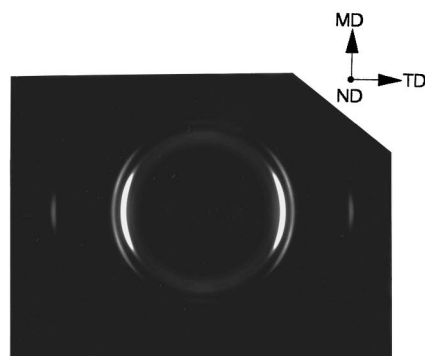


**FIG. 5.** (a) The TEM micrograph for resin 1, sample A1 showing no fibril nuclei. (b) The WAXS diffraction pattern for resin 1, sample A1 that did not possess fibril nuclei.

for resin 2. Therefore, a critical minimum orientation function may not be an essential requirement for the presence of fibril nuclei. The TEM micrographs and WAXS diffraction patterns for the lowest and highest oriented extruded films made from resin 1, samples A1, and A10, are shown in Figs. 5 and 6, respectively. The highly oriented fibril nuclei are not evident in Figs. 5(a) and 6(a) and nor were there sharp spots along the WAXS diffraction equator, which would arise from fibril nuclei as observed earlier for resin 2 seen in Figs. 5(b) and 6(b). Only the broader azimuthal spreading reflections, originating from the stacked lamellar structure, were clearly observed in the WAXS diffraction patterns for samples A1 and A10. This observation indicates that either the highly oriented fibril nuclei do not exist in the resin 1 extruded films A1 and A10 or the concentration of the fibril nuclei is too small in the two samples to be detected by TEM and WAXS. In our previous paper, we proposed that the cause of the difference in the morphological textures of the extruded films of resins 1 and 2 was promoted by the difference in their melt relaxation time behavior under equal processing conditions. The rheological results discussed earlier in the present paper clearly show that at the same melt temperature, resin 2 possesses a much longer relaxation time than resin 1. This observation suggests that when the polymer melt flows through the die, under the same melt processing conditions, resin 2 can obtain a higher orientation state in the melt that promotes a greater crystallization rate as predicted by Ziabicki (1974), (1978). A faster



(a)



(b)

**FIG. 6.** (a) The TEM micrograph for resin 1, sample A10 showing no fibril nuclei. (b) The WAXS diffraction pattern for resin 1, sample A10 that did not possess fibril nuclei.

crystallization rate and longer melt relaxation time behavior allow resin 2 to relax slower upon cooling than resin 1 and enhance the formation of highly oriented fibril nuclei. This also explains the difference between resins 1 and 2 for their morphological characteristics developed under the same processing conditions.

Since the melt relaxation behavior can also be influenced by extrusion processing variables, if one can shorten the melt relaxation time of resin 2 and/or increase the process time frame of the cooling step, one should be able to produce extruded film without prominent fibril nuclei from resin 2. In order to verify this concept, a new film of resin 2 (sample B12) was processed with a higher melt temperature (210 °C), a greater quench height (3.5 in.), a lower quench rate, and a slower line speed, and compared to sample B1 {variables outside the range utilized in our previous work [Yu and Wilkes (1996)]}. The corresponding TEM micrograph and WAXS diffraction pattern for sample B12 are shown in Figs. 7(a) and 7(b), respectively. In this sample, no distinct intense sharp spots were observed on the (110), (200), and (020) reflections along the equatorial direction in Fig. 7(b). Also no sign of fibril nuclei are seen of the TEM micrograph in Fig. 7(a). Comparing these results (sample B12) to those from the earlier extruded films made from resin 2 in our previous work, sample B12 also has the lowest orientation function value ( $f_c = 0.47$ ). Since the melt relaxation time of resin 2 is strongly dependent on the

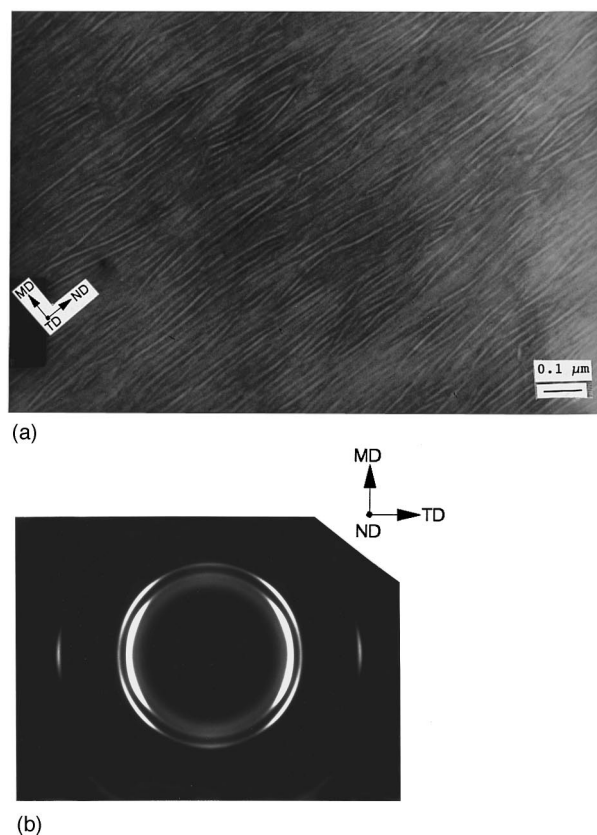


**FIG. 7.** (a) The TEM micrograph for resin 2, sample B12 showing no fibril nuclei. (b) The WAXS diffraction pattern for resin 2, sample B12 that did not possess fibril nuclei.

processing temperature, a higher melt temperature (210 °C) can significantly shorten its melt relaxation time at the die exit. On the other hand, a greater quench height (3.5 in.), a lower quench rate, and a slower line speed also give a longer processing time frame for the polymer melt to relax more during the cooling/solidification process. Therefore, sample B12 has a lower orientation state than the other samples made from resin 2 and less chance to form highly oriented fibril nuclei. This example nicely displays the influence of relaxation behavior of an oriented polymer melt during the cooling and crystallization process on structure development (such as orientation and the formation of fibril nuclei) in the extruded films.

The presence of fibril nuclei structure has been noticed to be important for enhancing the mechanical performance of PE fibers, i.e., promoting a higher modulus. In order to find out if there is any influence of fibril nuclei on the mechanical properties of extruded films, the highest oriented resin 2 (sample B11, which possesses fibril nuclei) studied in our previous work and sample B12 without fibril nuclei were characterized by tensile testing. A direct comparison of the stress–elongation behavior for the two samples is shown in Fig. 8. Note that the modulus and the strength are distinctly higher and the ultimate strain is lower for sample B11, which possesses a significant prevalence of fibril nuclei. The difference for the average values of these three properties between samples B11 and B12 is presented in Table III. It was noted in Table III that the modulus and

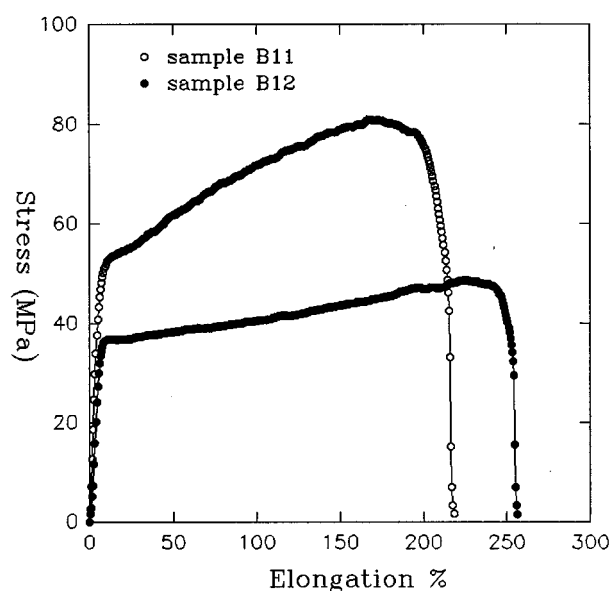


FIG. 8. The stress–elongation curves for samples B11 and B12 as measured along the machine direction.

strength of sample B11 were 20% and 30% greater than those of sample B12, respectively. The elongation% at break for sample B11 was 25% less than that of sample B12. These results suggest, as might be expected, that the fibril nuclei structure play a role in determining the mechanical response of these extruded films. Since sample B11 has a higher orientation state ( $f_c = 0.72$  vs  $f_c = 0.45$ ) than sample B12, there is also a potential influence from the orientation on their mechanical responses. Therefore, it would be interesting to further investigate the separate effect of the two factors (orientation and fibril nuclei structure) on the mechanical performance of oriented extruded films.

As described earlier, for the same processing window utilized for resin 2 in our previous study, none of the extruded films made from resin 1 showed fibril nuclei.

TABLE III. Summary of mechanical properties for samples B11 and B12 as measured along the machine direction.

Sample No.	Test No.	$E$ (MPa)	Strength (MPa)	Elongation % at break
B11	1	1016	80	166
	2	965	84	177
	3	1006	84	181
	4	1069	81	196
	5	1024	80	160
	average		$1016 \pm 37$	$82 \pm 2$
B12	1	776	50	240
	2	831	53	232
	3	810	50	233
	4	772	49	240
	5	839	51	215
	average		$806 \pm 31$	$51 \pm 2$

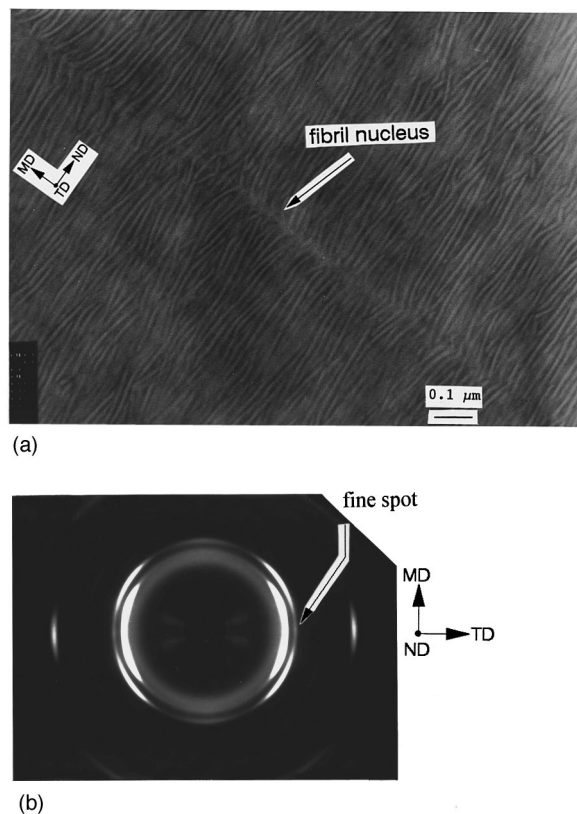


**FIG. 9.** (a) The TEM micrograph for resin 1, sample A11 showing fibril nuclei. (b) The WAXS diffraction pattern for resin 1, sample A11 that possessed fibril nuclei.

However, as just demonstrated, extruded film of resin 2 (sample B12), which does not show fibril nuclei, was successfully prepared by choosing the appropriate extrusion processing conditions to alter the crystallization–melt relaxation behavior. This observation strongly suggests the possibility that one might be able to also generate the observance of fibril nuclei in resin 1 by again tuning the processing conditions to promote solidification of suitably oriented melt of this resin. For the purpose of promoting the fibril nucleated structure for resin 1, the extruded film, sample A11, was processed with a smaller quench height (1.0 in. vs 3.5 in.), a lower melt temperature (185 °C vs 210 °C), a faster quench rate, a higher line speed (80 ft/min vs 40 ft/min), and a thicker die gap (0.14 in. vs 0.07 in.) but the same final film thickness. Figures 9(a) and 9(b) show the respective TEM micrograph and WAXS diffraction pattern for sample A11 made from resin 1. The fine intense spots, which were too weak to be clearly seen on the (110) and (020) reflections, were, however, distinctly observed on the (200) reflection along the equator in the WAXS diffraction pattern [Figure 9(b)]. The distinct intense fine equatorial spot on the (200) reflection clearly suggests that there is a low concentration of fibril nuclei in sample A11 and this is directly supported by the fibril nucleus being observed in the TEM micrograph of Fig. 9(a).

Comparing the processing conditions for samples A10 and A11, it is also noted that a thicker die gap can enhance the formation of fibril nuclei for the extruded film (such as sample A11) made from resin 1. As the oriented polymer melt was drawn out of the die,

it formed the extruded film having the same thickness of 1 mil. The transformation mechanism from the melt in the die to the extruded film with 1 mil thickness at the die exit is actually equivalent to a drawing process with a draw-down ratio defined by the ratio of the die gap to the film thickness. At a constant film thickness, a thicker die gap requires a greater draw-down ratio, which in turn enhances the formation of the highly oriented fibril nuclei in sample A11. These observations clearly show that the extruded film with or without the direct observation of fibril nuclei can be produced for both resins with different molecular weight characteristics (possessing different melt relaxation time behavior at a given temperature) by tuning the processing variables correctly.

The coil  $\rightarrow$  stretching transition concept proposed by de Gennes (1974) has been applied by Keller *et al.* (1993) to explain the orientation phenomena in polymer melt during processing and their consequence for structure formation. Keller *et al.* suggested that the polymer chain orientation caused by melt flow during processing are of two types of orientation: the essentially fully stretched out and the essentially unoriented random chain, with no intermediate status. When passing from the melt to the crystalline state, the random chains lead to chain folded lamellae and the extended chains to fibril nuclei with the chains nearly essentially extended within them. Intermediate orientation states obtained in the final product were speculated to be due to the different combinations of the two extremes. The mechanism of forming fibril nuclei in extruded films was investigated in this paper as well as in our previous reported work. The results obtained in our studies indicate that the melt relaxation mechanism is important for the structure formation in the extruded films. A longer melt relaxation time and a shorter processing time frame upon cooling can enhance the formation of fibril nuclei. Intense sharp equatorial reflections were not seen in the WAXS diffraction patterns of the extruded films in which fibril nuclei were not evident by TEM. Since this observation suggests that the concentration of fibril nuclei in these samples is either null or extremely small, the contribution of orientation from the fully stretched chains in these extruded films may not be significant. For the samples that possess fibril nuclei, the highly oriented fibril nuclei confirmed by the intense sharp equatorial reflections in the WAXS diffraction patterns can be separated from the other oriented stacked lamellar matrix that causes the broader azimuthal spreading of the WAXS reflections. It is, therefore, clear that the folded chains in the oriented stacked lamellar matrix also possess a certain level of orientation. In contrast to the coil  $\rightarrow$  stretching model, the results presented in this paper suggest that the state of orientation produced in the final extruded films is not necessarily only a combination of the two extremes described above but rather may possibly arise from oriented chains possessing intermediate orientation states. Clearly, further investigations addressing this important subject are warranted.

#### IV. SUMMARY AND CONCLUSIONS

In this study, it was shown that the melt relaxation behavior can be controlled by varying the melt process conditions to produce extruded films with and without the direct observation of fibril nuclei for each of the two HDPE resins utilized. Rheological analysis showed that the melt relaxation time obtained from a Carreau–Yasuda analysis for resin 2 that possesses a broader molecular weight distribution was 6.5 times greater than that of resin 1, the latter of which has a narrower molecular weight distribution. These observations confirm what was suggested in our previous work. Specifically, the melt relaxation behavior during the melt cooling and solidification process is particularly important in determining if fibril nucleated structure will develop. These observations also suggest that the single characteristic relaxation time obtained from the Carreau–Yasuda model

can be a useful guide in the selection of HDPE or likely other resin and for optimizing extrusion processing variables to obtain the desired structure–orientation–property response in extruded films.

## ACKNOWLEDGMENTS

The authors wish to acknowledge the financial support of this work by the Hoechst Celanese Corporation. In addition, the authors would like to thank Jay Janzen and Michael Hicks for their assistance regarding the rheological experiments and their valuable suggestions.

## References

- Bashir, Z., J. A. Odell, and A. Keller, "Stiff and strong polyethylene with shish kebab morphology by continuous melt extrusion," *J. Mater. Sci.* **22**, 3993–4002 (1986).
- Bird, R. B., R. C. Armstrong, and O. Hassager, *Dynamics of Polymeric Liquids* (Wiley, New York, 1987), Vol. 1, pp. 139–143.
- Callahan, R. W. and H. M. Fisher (private communication).
- Cantow, H. J., "The influence of molecular-weight distribution on the melt-flow properties of polystyrenes," *Plast. Inst. Trans. J.* **31**, 141–145 (1963).
- de Gennes, P. G., "Coil-stretch transition of dilute flexible polymers under ultrahigh velocity gradients," *J. Chem. Phys.* **60**, 5030–5042 (1974).
- Friedman, E. M. and R. S. Porter, "Polymer viscosity-molecular weight distribution correlations via blending: For high molecular weight poly(dimethyl siloxanes) and for polystyrenes," *Trans. Soc. Rheol.* **19**, 493–508 (1975).
- Graessley, W. W., "Molecular Entanglement Theory of Flow Behavior in Amorphous Polymers," *J. Chem. Phys.* **43**, 2696–2703 (1965).
- Graessley, W. W., "Viscosity of Entangling Polydisperse Polymers," *J. Chem. Phys.* **47**, 1942–1953 (1967).
- Graessley, W. W., "The Entanglement Concept in Polymer Rheology," *Adv. Polym. Sci.* **16**, 70–99 and 132–148 (1974).
- Grubb, D. T. and A. Keller, "Lamellar Morphology of Polyethylene: Electron Microscopy of a Melt-Crystallized Sharp Fraction," *J. Polym. Sci., Polym. Phys. Ed.* **18**, 207–216 (1980).
- Hermans, P. H., J. J. Hermans, D. Vermaas, and A. Weidinger, "Deformation Mechanism of cellulose gels IV. General relationships between orientation of the crystalline and that of the amorphous portion," *J. Polym. Sci.* **3**, 1–9 (1948).
- Keller, A. and J. W. H. Kolnaar, "Chain extension and orientation: Fundamentals and relevance to processing and products," *Progress Colloid Polym. Sci.* **92**, 81–102 (1993).
- Misra, S., Lu, F. M., J. E. Spruiell, and G. C. Richeson, "Influence of Molecular Weight Distribution on the Structure and Properties of Melt-Spun Polypropylene Filaments," *J. Appl. Polym. Sci.* **56**, 1761–1779 (1995).
- Shaw, M. T., "Melt Characterization of Ultrahigh Molecular Weight Polyethylene Using Squeeze Flow," *Polym. Eng. Sci.* **17**, 266–268 (1977).
- Shroff, R. N. and A. M. Shida, "Correlation between Steady State Flow Curve and Molecular Weight Distribution for Polyethylene Melts," *Polym. Eng. Sci.* **11**, 200–204 (1971).
- Stein, R. S., "The X-Ray Diffraction, Birefringence, and Infrared Dichroism of Stretched Polyethylene. II. Generalized Uniaxial Crystal Orientation," *J. Polym. Sci.* **31**, 327–334 (1958).
- Stein, R. S., "The X-Ray Diffraction, Birefringence, and Infrared Dichroism of Stretched Polyethylene. III. Biaxial Orientation," *J. Polym. Sci.* **31**, 335–343 (1958).
- Stein, R. S., "Optical Methods of Characterizing High Polymers," *Newer Methods in Polymer Characterization* (Wiley-Interscience, New York, 1964), Chap. IV.
- Tanner, R. I., *Engineering Rheology* (Clarendon, Oxford, 1988), p. 353.
- Vinogradov, G. V. and A. Y. Malkin, *Rheology of Polymers* (Springer-Verlag, Berlin, 1980), pp. 153–182, pp. 118–119.
- Wilkes, G. L., "An Overview of the Basic Rheological Behavior of Polymer Fluids with an Emphasis on Polymer Melts," *J. Chem. Education* **58**, 880–892 (1981).
- Yasuda, K., R. C. Armstrong, and R. E. Cohen, "Shear flow properties of concentrated solutions of linear and star branched polystyrenes," *Rheol. Acta* **20**, 163–178 (1981).

- Yu, T. H. and G. L. Wilkes, "Orientation Determination and Morphology Study of High Density Polyethylene (HDPE) Extruded Tubular Films: Effect of Processing Variables and Molecular Weight Distribution," *Polymer* (in press).
- Ziabicki, A., "Theoretical analysis of oriented and nonisothermal crystallization I. Phenomenological considerations, isothermal crystallization accompanied by simultaneous orientation or disorientation," *Colloid Polym. Sci.* **252**, 207–221 (1974).
- Ziabicki, A., "Theoretical analysis of oriented and non-isothermal crystallization II. Extension of the Kolmogoroff-Avrami-Evans theory onto processes with variable rates and mechanisms," *Colloid Polym. Sci.* **252**, 433–447 (1974).
- Ziabicki, A., "Theoretical analysis of oriented and non-isothermal crystallization III. Kinetics of crystal orientation," *Colloid Polym. Sci.* **256**, 332–342 (1978).